Light absorption and scattering

by high light-tolerant, fast-growing *Chlorella vulgaris* IPPAS-C1 cells

Barbora Baránková[a,b], Dušan Lazár[a,*], Jan Nauš[a], Alexei Solovchenko[c,d,e], Olga Gorelova[c], Olga Baulina[c], Gregor Huber[b], Ladislav Nedbal[b]

[a]Department of Biophysics, Centre of the Region Haná for Biotechnological and Agricultural Research, Faculty of Science, Palacký University, Šlechtitelů 27, 783 71 Olomouc, Czech Republic

[b]Institute of Bio- and Geosciences/Plant Sciences (IBG-2), Forschungszentrum Jülich, Wilhelm-Johnen-Straße, D-52428 Jülich, Germany

[c]Faculty of Biology, Moscow State University, Leninskie Gori 1/12, 119234, GSP-1, Moscow, Russia

[d]Peoples Friendship University of Russia (RUDN University), Moscow, 117198, Russia

[e]Pskov State University, Pskov, 180000, Russia

*Corresponding author:

Dušan Lazár, e-mail: dusan.lazar@upol.cz

Abstract

Algal cells are highly complex optical systems that can dynamically change their structure. Consequently, absorption and scattering properties of algae change, while the cells are acclimating to different light conditions or during growth and division in a cell cycle. This may be particularly important in algal species that can grow rapidly under very high-light such as *Chlorella vulgaris* IPPAS-C1 that is studied here. From cell transmittance measured conventionally and using integrating sphere, we evaluated absorption and scattering coefficients and cross sections per cell dry weight and chlorophyll content. This was done for asynchronous cell culture grown in low-light (LL; 220 μmol (photons) m^{-2} s^{-1}) or high-light (HL; 1760 μmol (photons) m^{-2} s^{-1}) light, as well as during cell cycle of synchronous culture grown in HL. During the cell cycle, we also determined cell ultrastructural organization by transmission electron microscopy, and correlated its parameters with absorption and scattering cross sections per cell dry weight. We found that the IPPAS-C1 cells of asynchronous culture scatter light more than other cells, however, internal organization of the cells that is decisive for scattering is less sensitive to HL and LL treatment than the cell pigment content that controls absorption. The light scattering and absorption were dynamically changed during cell cycle of synchronous cells grown in the HL. Changes in ratio of chloroplast to protoplast area, reflecting amount of scattering chloroplast membrane (outer, inner) interfaces, best correlated with changes in light scattering. We suggest that the increased light scattering by the HL-acclimated IPPAS-C1 cells might be responsible for increased HL resilience reported in the literature. Biotechnological aspect of this study is that the scattering and absorption properties of phytoplankton cells ought to be calibrated for each particular growth phase or irradiance to which the cells are acclimated.

Key words:

Cell wall, chloroplast; electron microscopy; periplasm; pigments; starch grains

Symbols (ordered by appearance in the text):

$T_{n,\lambda,susp}$ – normal-normal transmittance of algal cell suspension at wavelength λ that was measured by a conventional spectrophotometer using a collimated beam that was incident as a normal to 10 × 10 mm cuvette and with detection normal to the other side of the cuvette;

$T_{n,\lambda,ref}$ – normal-normal transmittance of the medium at wavelength λ that was measured as $T_{n,\lambda,susp}$;

$T_{n,\lambda,cells}$ – normal-normal transmittance of algal cells at wavelength λ calculated as $T_{n,\lambda,susp}/T_{n,\lambda,ref}$;

x – thickness of the optical cuvette, here 10 mm;

$\varepsilon_\lambda^\star$ – apparent sample extinction coefficient that reflects light attenuation in conventional spectrophotometer by both absorption and scattering. The word 'apparent' indicates that a correction for an incomplete forward scattering by the algal cells is required;

κ_λ − real absorption coefficient;

σ_λ − real scattering coefficient;

f_n − fraction of the forward-scattered light which is sensed by the detector in the conventional spectrophotometer;

$T_{h,\lambda,susp}$ – normal-hemispherical transmittance of the algal cell suspension at wavelength λ that was measured by LI 1800 spectrometer using a collimated beam that was incident as a normal to optical cuvette and with detection using an integrating sphere that collected forward-scattered photons;

$T_{h,\lambda,ref}$ – normal-hemispherical transmittance of the medium at wavelength λ that was measured as $T_{h,\lambda,susp}$;

$T_{h,\lambda,cells}$ – normal-hemispherical transmittance of algal cells at wavelength λ calculated as $T_{h,\lambda,susp}/T_{h,\lambda,ref}$;

$\kappa_\lambda^\star$ – apparent absorption coefficient;

f_h – fraction of the forward-scattered light which is sensed by the detector of the integrating sphere;

$A_{dw,\lambda}$ – absorption cross-section per unit algal cell dry weight;

$S_{dw,\lambda}$ – scattering cross-section per unit algal cell dry weight;

$A_{chlw,\lambda}$ – absorption cross-section per unit algal chlorophyll mass content;

$S_{chlw,\lambda}$ – scattering cross-section per unit algal chlorophyll mass content.

1. Introduction

The biomass productivity in algal photobioreactors is, for a given photosynthetically active irradiance (PAR), a product of specific growth rate and of the culture density (Aiba 1982, Droop 1983, Schreiber et al. 2017). The fast growing algal species thus offer an opportunity for achieving high biomass productivities in the photobioreactors, particularly if the fast growth is combined with tolerance to wide range of irradiances. Sorokin reported already in late 1950's that *Chlorella sorokiniana* can double more than 8 times per 24 hours (Sorokin 1959). Extremely high growth rates and high-light resilience for certain representatives of the genus *Chlorella* were recently reported (Treves et al. 2013, 2016). Interestingly, similar phenotype was found earlier also in an arctic location in Russia (Semenenko and Zvereva 1972) and in temperate zone in Germany (Böhm 1973), regions that vastly differ from subtropical USA as well as from the arid Negev desert in Israel where the other *Chlorella* species were found. *Chlorella vulgaris* IPPAS C-1 that is used also in the present study was isolated close to Dvina

river in northern Russia and its unique properties have been described in Semenenko and Zvereva (1972). Molecular mechanisms that are responsible for the high-light resilience are subject of intense research (Treves et al. 2016) and here we aim at contributing to this quest by investigating optical properties of *C. vulgaris* IPPAS C-1 as related with its ultrastructural organization.

The optical properties of algal cell and hence those of cell suspension also determine light distribution inside the algal photobioreactors, a factor that largely controls their biomass productivity (Schreiber et al. 2017). Interaction of light with algal cells includes absorption by pigments, mainly chlorophylls (chls) and carotenoids, and scattering by cellular structures. Here, scattering is meant to include any process that leads to change of photon direction that occurs without changing its energy. Some photons may be elastically scattered, e.g., on starch grains and some may change direction by reflection on numerous often stochastically oriented cellular interfaces that separate compartments with differing refractive indexes, such as cell wall/cytoplasm or organelle membrane(s)/cytoplasm. Knowledge of spectral light absorption and scattering properties of algal suspensions is required for analysis and modeling of light distribution inside photobioreactors and, thus, for knowledge-based analysis and modeling of algal growth (Wheaton and Krishnamoorthy 2012, Nauha and Alopaeus 2013, Kong and Vigil 2014, Huang et al. 2014, de Mooij et al. 2017, Fuente et al. 2017, 2018, Schreiber et al. 2017, Ma et al. 2019).

Optical properties of microalgal cells of different shapes and sizes have been often theoretically calculated and/or experimentally measured (Bricaud and Morel 1986, Pottier et al. 2005, Quirantes and Bernardt 2006, Berberoglu et al. 2007, 2008, 2009, Gaigalas et al. 2009, Heng et al. 2014, 2015, Dauchet et al. 2015, Bhowmik and Pilon 2016, Heng and Pilon 2014, 2016). Also effects of chl content on the spectral absorption and scattering coefficients have been explored using *Chlamydomonas reinhardtii* cells with truncated light harvesting antenna or

nitrogen-starved cells with a low chl content (Berberoglu et al. 2008, Kandillan et al. 2016a). Supporting information can be also obtained from reports on optical properties of isolated thylakoids or chloroplasts of higher plants (Paillotin et al. 1998, Merzlyak et al. 2009) and higher plants (Fukshansky and Kazarinova 1980, Seyfried and Fukshansky 1983, Lork and Fukshansky 1985, Ganapol et al. 1998, Berdnik et al. 2001, Sušila and Nauš 2007, Krekov et al. 2009, Watté et al. 2015, Baránková et al. 2016, Ho et al. 2016).

Here, we aim at deepening insight into the relationship between optical properties of algal cells, growth irradiance, and cell cycle. For that we quantified absorption and scattering coefficients and cross-sections of *Chlorella vulgaris* IPPAS C1 grown in limiting and saturating PAR levels and during its cell cycle and confronted the results with the characteristic changes in the ultrastructure of the algal cell.

2. Material and methods

2.1 Algae

Chlorella vulgaris IPPAS C1 was obtained from the culture collection of the K.A. Timiryazev Institute of Plant Physiology—IPPAS, Russian Academy of Science (courtesy of M. Sinetova). The strains were maintained on agar slants enriched with Tris-Acetate-Phosphate nutrient medium (Gorman and Levine 1965) in the laboratory at a light intensity of about 50 μmol m^{-2} s^{-1}, 16/8 h (light/dark) regime and temperature of 28 °C. Experimental cultures were prepared by transfer of algae from the agar slants into liquid Tris-Acetate-Phosphate medium and pre-cultured in 1000 ml Erlenmeyer flasks. The nutrient medium composition was derived from the chemical composition of the microalgal biomass according to Douskova et al. (2009) and consisted of the following in mM: 18.32 $(NH_2)_2CO$, 1.74 KH_2PO_4, 0.83 $MgSO_4.7H_2O$, 0.79 $CaCl_2$, 0.11 FeNa-$C_{10}H_{12}O_8N_2$, 0.017 $MnCl_2.4H_2O$, 0.013 H_3BO_3, 0.009 $ZnSO_4.7H_2O$, 0.004 $CuSO_4.5H_2O$, 0.002 $CoSO_4.7H_2O$, 0.0001 $(NH_4)_6Mo_7O_{24}.4H_2O$ and 0.0001 $(NH_4)VO_3$ made

up in domestic tap water. At this concentration, the medium is supposed to yield up to 6 g (dw) l^{-1} *Chlorella* biomass before being limited by nutrients.

Cultivations were done in photobioreactors FMT150 (PSI, Brno, Czech Republic) as described in Nedbal et al. (2008). The algae were grown at 35 °C, which was found to be an optimum temperature (data not shown), in pH 7–8, and in different irradiance levels generated equally by sets of red and blue light emitting diodes (Nedbal et al. 2008). The maximal available PAR irradiance (100%) was ca. 2200 μmol (photons) m^{-2} s^{-1} and the cell grew under either 80% of maximum irradiance (1760 μmol (photons) m^{-2} s^{-1}; high-light conditions; HL) or 10% of maximum irradiance (220 μmol (photons) m^{-2} s^{-1}; low-light conditions; LL). As shown in Schreiber et al. (2017), the HL irradiance safely saturated growth while LL reduced growth by energetically limiting photosynthesis. To study optical properties during the cell cycle, the cells grew under the HL conditions.

The suspension was bubbled with air enriched by 1% (v/v) CO_2 with gas flow rate 0.5 l min^{-1} through 1-litre suspension volume. The suspension was diluted daily to constant absorbance (optical density) measured at 680 nm (OD_{680}).

Dry weight of the algal suspension was determined gravimetrically. Suspension aliquots of 10 ml were vacuum-filtrated through pre-washed and weighed 25 mm Whatman GF/C glass fiber filters. The filters with algae were dried for 2 hours at 105 °C. The dry weight of the algal cells was determined as the difference between the weight of the dried filter with algal biomass and the weight of the dry filter before the filtration. The dry weight was determined from three samples.

The algal suspension was further characterized by counting cells per volume and by determining their size distribution in the particle counter Multisizer 3 (Beckman Coulter, Krefeld, Germany).

For pigment analysis, the algae were centrifuged for 5 min at 7 000 g (4 °C) in 5430R centrifuge (Eppendorf, Germany). The pellet was diluted in cold 80% acetone prepared by adding 0.2 ml of 5% w/v $NaCO_3$ to 0.8 ml of 100% acetone. The suspension was vortexed until the pellet was re-suspended and, then, hard ceramic beads (YZ, 3-3.3 mm, SoilGEN, Aachen, Germany) were added and vortexes again until the algal cells were broken up. The suspension of broken up cells was centrifuged for 5 min at 20 000 g (4 °C). The resulted supernatant was used for spectrophotometric determination of chl (a + b) and total carotenoid concentrations according to Lichtenthaler (1987). The samples were on ice during the measurements. The pigment analysis was determined from three samples.

2.2 Transmission electron microscopy

The microalgae samples for transmission electron microscopy (TEM) were prepared according to the standard protocol involving fixation in 2.5 % v/v glutaraldehyde in the cultivation medium and post-fixation for 4 h in 1% (w/v) OsO_4 in 0.1 M sodium cacodylate buffer (pH 6.8–7.2, depending on the culture pH) at room temperature for 0.5 h. The samples, after dehydration through graded ethanol series including anhydrous ethanol saturated with uranyl acetate, were embedded in araldite. Ultrathin sections were made with an LKB-8800 (LKB, Sweden) ultratome, mounted to the formvar-coated TEM grids, stained with lead citrate (Reynolds 1963) and examined under JEM-1011 (JEOL, Tokyo, Japan) microscope.

Quantitative morphometric analysis was carried out as described earlier in detail in Gorelova et al. (2015). Namely, the organelles were counted on the sections through the cell equator or subequator with at least ten samples from each treatment examined. Probabilities of finding a particular structure were calculated as a ratio of the number of cell sections containing the structure of interest to total number of cell sections made. Linear and areal sizes were measured on the TEM micrographs of the cell ultrathin sections (20 cell sections were analyzed in each

case; at least 32 size measurements have been carried out on each morphological parameter of the cell) using ImageJ software (NIH, Bethesda MA, USA).

2.3 Absorption and scattering of light by algae

The method (Bricaud et al. 1983, Davies-Colley 1983, Davies-Colley et al. 1986, Pilon et al. 2011, Pilon and Kandilian 2016) starts with measuring light transmittance through a cuvette with algal suspension using a conventional spectrometer, i.e., with a collimated light and with detection oriented selectively towards the incident beam. In this configuration, most of scattered photons escape the narrow-angle detection. The second measurement is done with an integrating sphere which broadly collects photons that pass through the sample cuvette, including those that are scattered to different angles in the forward hemisphere. The transmissions measured with and without the integrating sphere are recorded for different photon wavelengths and interpreted assuming (Berberoglu et al. 2007, 2008) that each photon is, during the sample cuvette passage, absorbed by algal pigments or transmitted without scattering or scattered once preferentially in the forward direction as anticipated largely for the Lorenz-Mie type scattering (e.g., Kerker 1982, Uličný 1992).

With these assumptions, the sample normal-hemispherical transmittance spectrum $T_{h,\lambda}$ quantifies exclusively photon absorption and, thus, can be re-calculated into apparent sample absorption coefficient $\kappa_\lambda^\star$. In contrast, the sample normal-normal transmittance $T_{n,\lambda}$ that is measured with a conventional spectrometer detects light only with a small acceptance angle and, thus, the detected light is attenuated by both, the light absorption and the light scattering. Consequently, the $T_{n,\lambda}$ spectrum yields the apparent sample extinction coefficient $\varepsilon_\lambda^\star$ that combines attenuation by both absorption and scattering.

The apparent extinction spectrum $\varepsilon_\lambda^\star$ was measured by the spectrometer UviconXL (Bio-tek Instrumental, Milano, Italy) that compared the normal-normal transmittance spectra of

reference (growth medium only) without algae $T_{n,\lambda,ref}$, to the one found with algal suspension $T_{n,\lambda,susp}$:

$$\varepsilon_\lambda^\star = -\frac{1}{x}\ln\frac{T_{n,\lambda,susp}}{T_{n,\lambda,ref}}\,, \tag{1}$$

where x was the cuvette geometrical thickness, here 10 mm. The ratio $T_{n,\lambda.susp}/T_{n,\lambda.ref}$ characterizes normal-normal transmittance of agal cells alone, $T_{n,\lambda.cells}$. To compare the $T_{n,\lambda.susp}$ and $T_{n,\lambda.ref}$ spectra with equivalent spectra measured with a spectrometer equipped with an integrating sphere, where cuvette with geometrical thickness of 5 mm (and also 2 and 1 mm) was used (see below), the $T_{n,\lambda,susp}$ and $T_{n,\lambda,ref}$ spectra were recalculated for 5 mm and the $T_{n,\lambda,susp}$ spectra for cuvette with geometrical thickness of 5 mm are shown in Figs. 1 and 5.

The thus determined apparent extinction spectrum $\varepsilon_\lambda^\star$ is a function of the real absorption coefficient κ_λ and of the real scattering coefficient σ_λ with a correction for incomplete forward scatter:

$$\varepsilon_\lambda^\star = \kappa_\lambda + (1 - f_n)\,\sigma_\lambda, \tag{2}$$

Here, f_n is the fraction of the forward-scattered light which is sensed by the detector. The f_n is assumed to be constant in the visible light range and its value can be estimated from the scattering phase function $\Phi_{T,\lambda}(\theta)$ of the given algal suspension as:

$$f_n = \frac{1}{2}\int_0^{\theta_a} \Phi_{T,\lambda}(\theta)\sin(\theta)\,d\,\theta, \tag{3}$$

where θ_a is the half acceptance angle of the detector. An estimate $f_n \approx 0.7$ can be obtained when considering θ_a of the spectrometer 5° and using the Henyey-Greenstein phase function (Henyey and Greenstein 1941) for approximation of $\Phi_{T,\lambda}(\theta)$ with assumed value of anisotropy factor g 0.97 (similar to 0.979 reported for *Chlorella sp*. by Berberoglu et al. (2009)).

In this approximation, Eq. (2) yields:

$$\varepsilon_\lambda^\star \approx \kappa_\lambda + 0.3\,\sigma_\lambda, \tag{4}$$

which relates to the real extinction coefficient $\varepsilon_\lambda \equiv \kappa_\lambda + \sigma_\lambda$ as:

$$\varepsilon_\lambda = (\varepsilon_\lambda^\star - 0.7\,\kappa_\lambda)/0.3. \quad (5)$$

The apparent absorption spectrum $\kappa_\lambda^\star$ is obtained analogously using the spectrometer LI-1800 with the integrating sphere LI-1800-12 (LI-COR, Lincoln, USA) instead of the conventional spectrophotometer. The measurement yields the normal-hemispherical transmittance spectra of the reference (growth medium only) without algae, $T_{h,\lambda,ref}$, and of the algal suspension, $T_{h,\lambda,susp}$ that are used to calculate $\kappa_\lambda^\star$:

$$\kappa_\lambda^\star = -\frac{1}{x}\ln\frac{T_{h,\lambda,susp}}{T_{h,\lambda,ref}}. \quad (6)$$

The ratio $T_{h,\lambda.susp}/T_{h,\lambda.ref}$ characterizes normal-hemispherical transmittance of agal cells alone, $T_{h,\lambda.cells}$. The $T_{h,\lambda.susp}$ spectra for given sample and $T_{h,\lambda.ref}$ spectra of the reference were measured two times, in cuvettes with 2 mm and with 5 mm geometrical thickness in case of the HL *vs* LL experiment and three times, in cuvettes with 1, 2, and 5 mm geometrical thickness in case of the cell cycle experiment. The spectra of evaluated κ_λ and σ_λ were the same if based on the spectra measured with 1-, 2- or 5-mm-cuvette but spectra based on 5-mm-cuvette measurements had the lowest noise, thus only spectra based on 5-mm-cuvette measurements were used for presentations in the figures.

The real absorption spectrum κ_λ is related to the spectra of $\kappa_\lambda^\star$ and σ_λ by:

$$\kappa_\lambda^\star = \kappa_\lambda + (1 - f_h)\,\sigma_\lambda, \quad (7)$$

where f_h is the fraction of the forward-scattered light, which is detected by the detector of the integrating sphere. Absorption of green algae at 750 nm is negligible ($\kappa_{750} = 0$) and, thus, f_h can be calculated from Eq. (7) when knowing $\kappa_{750}^\star$ and σ_{750}. With this substitution ($f_h = 1 - \kappa_{750}^\star/\,\sigma_{750}$), Eq. (7) yields relationship between the real κ_λ and apparent $\kappa_\lambda^\star$ absorption spectra:

$$\kappa_\lambda = \kappa_\lambda^\star - \kappa_{750}^\star\frac{\sigma_\lambda}{\sigma_{750}}. \quad (8)$$

The ratio $\frac{\sigma_\lambda}{\sigma_{750}}$ can be derived by subtracting Eq. (7) from Eq. (2) for arbitrary λ and λ = 750 nm and by putting the expressions for σ_λ for arbitrary λ and λ = 750 nm in a ratio:

$$\frac{\sigma_\lambda}{\sigma_{750}} = \frac{(\varepsilon^\star_\lambda - \kappa^\star_\lambda)}{(\varepsilon^\star_{750} - \kappa^\star_{750})}. \quad (9)$$

Substituting further from Eq. (9) into Eq. (8), one obtains:

$$\kappa_\lambda = \kappa^\star_\lambda - \kappa^\star_{750} \frac{(\varepsilon^\star_\lambda - \kappa^\star_\lambda)}{(\varepsilon^\star_{750} - \kappa^\star_{750})}. \quad (10)$$

Equation (10) allows calculating the real absorption coefficient κ_λ from the apparent absorption coefficients $\kappa^\star_\lambda$ and $\kappa^\star_{750}$ that are measured with the integrating sphere and from the apparent extinction coefficients $\varepsilon^\star_\lambda$ and $\varepsilon^\star_{750}$ that are measured in the conventional spectrophotometer, i.e., without the integrating sphere.

Having the real absorption coefficient κ_λ from Eq. (10) and the real extinction coefficient ε_λ from Eq. (5), one can calculate the real scattering coefficient σ_λ as their difference:

$$\sigma_\lambda = \varepsilon_\lambda - \kappa_\lambda. \quad (11)$$

Dimension of these coefficients is m^{-1} and as such characterize both algal cells as well as culture density.

With a reduced dependence on culture density, the absorption and scattering cross-sections per algal dry weight, $A_{dw,\lambda}$, $S_{dw,\lambda}$, respectively are than obtained from:

$$A_{dw,\lambda} = \frac{\kappa_\lambda}{\rho_{dw}} \text{ and } S_{dw,\lambda} = \frac{\sigma_\lambda}{\rho_{dw}}, \quad (12)$$

where ρ_{dw} is dry weight per sample volume. Similarly, the absorption and scattering cross-sections per chl weight, $A_{chlw,\lambda}$, $S_{chlw,\lambda}$, respectively are then obtained from:

$$A_{chlw,\lambda} = \frac{\kappa_\lambda}{\rho_{chlw}} \text{ and } S_{chlw,\lambda} = \frac{\sigma_\lambda}{\rho_{chlw}}, \quad (13)$$

where ρ_{chlw} is density of chls, i.e., chl a + b weight per sample volume (see above and Table 1).

3. Results and discussion

3.1 Optical properties of Chlorella cultures acclimated to saturating and limiting light levels

C. vulgaris IPPAS C1 was grown under continuous light, with PAR irradiance of 1760 μmol (photons) m^{-2} s^{-1} (high-light, HL) or 220 μmol (photons) m^{-2} s^{-1} (low light, LL). As shown

earlier by Schreiber et al. (2017), the growth was saturated by light in HL and light-limited in LL. The culture was diluted daily, and the stable conditions eliminated after 2–3 days any apparent synchronization of algal cells as shown by the distribution of cells diameters in Fig. S1 (Supplementary materials). Properties of algal cells and suspensions acclimated to HL and LL levels are listed in Table 1.

Table 1. Properties of *C. vulgaris* cells acclimated to 1760 µmol (photons) m^{-2} s^{-1} (high-light) or 220 µmol (photons) m^{-2} s^{-1} (low-light). The numbers represent mean values and the variance stands for standard deviation (n=3).

	Parameter	**High-light culture**	**Low-light culture**
Suspension	Dry weight density, 10^{-3} g(dw) L^{-1}	340 ± 20	230 ± 10
	Chl concentration, 10^{-3} g (Chl *a* + *b*) L^{-1}	4.2 ± 0.5	3.7 ± 0.2
	Chl *a* + *b*/dw 10^{-3} g (Chl *a* + *b*) / g (dw)	12 ± 5	16 ± 1
	Cell number / L, 10^{9} cells L^{-1}	26.3 ± 0.4	30.5 ± 0.2
Cell	Cell diameter, 10^{-6} m	3.58 ± 0.01	3.20 ± 0.01
	Cell volume, 10^{-15} L	30.0 ± 0.4	18.6 ± 0.1
	Dry weight per cell, 10^{-12} g (dw)/cell	12.9 ± 0.7	7.5± 0.1
	Chl per cell 10^{-12} g (Chl *a* + *b*)/cell	0.16 ± 0.03	0.12 ± 0.01

Suspensions of *C. vulgaris* cells acclimated to HL and LL levels were further characterized by normal-normal transmittance spectra $T_{n,\lambda,susp}$, and by normal-hemispherical transmittance spectra $T_{h,\lambda,susp}$ shown in Fig. 1. The spectra (and related absorbance spectra, see below) characterize whole alga suspensions, i.e., the algal cells in the growth medium, which is important for consideration of light intensity inside a photobioreactor. However, the used methodology considers transmittance signals of algal cells alone ($T_{n,\lambda,cells}$, $T_{h,\lambda,cells}$, see Material and methods), which are higher (see Fig. S2, Supplementary materials) than $T_{n,\lambda,susp}$ and $T_{h,\lambda,susp}$.

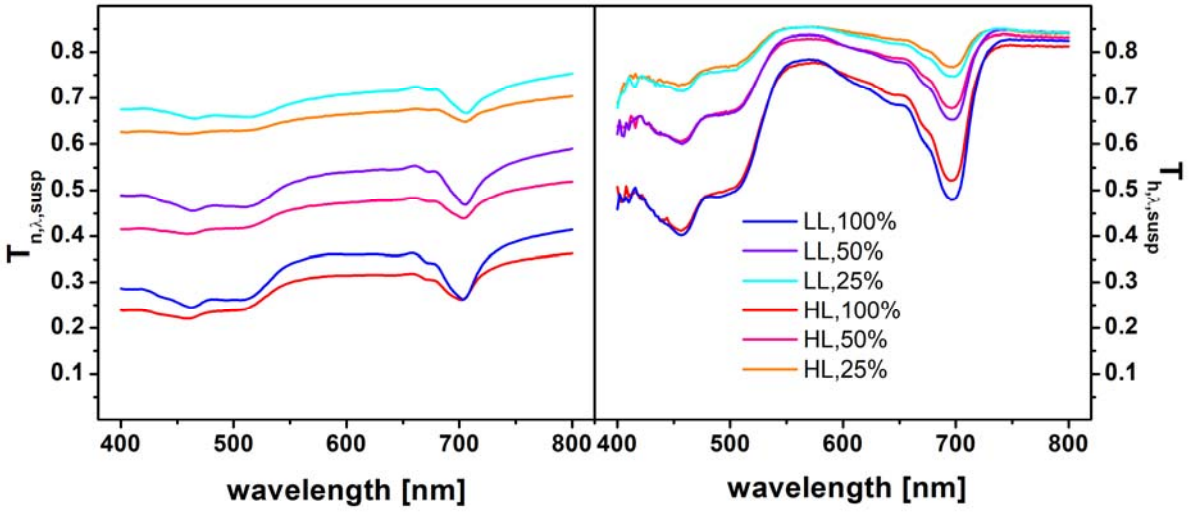

Figure 1. The normal-normal and normal-hemispherical transmittance spectra, $T_{n,\lambda,susp}$ and $T_{h,\lambda,susp}$, respectively, of the LL and HL acclimated algal cell suspensions measured for three different algal suspension dilutions. 100% corresponded to 0.34 ± 0.02 g(dw) L^{-1} in the HL culture and to 0.23 ± 0.01 g(dw) L^{-1} (mean ± standard deviation, n=3) in the LL culture. The spectra show transmittance at 5 mm (see Material and methods).

The spectra are, in general, a non-linear function of culture concentration (Nauš et al. 2018). To check how strong the non-linearity was, the spectra presented in Fig. 1 were measured without dilution (100%) as well as with twofold (50%) and fourfold (25%) dilutions. For a reference, the corresponding normal-normal absorbance spectra of $D_{n,\lambda,susp}$ and $D_{n,\lambda,cells}$ are shown in Figs. S3 and S4 (Supplementary materials), respectively. It is interesting to compare the results of the conventional spectrophotometer (Fig. 1, left panel) with the spectra obtained with an integrating sphere (Fig. 1, right panel). The spectra measured with the integrating sphere are a good proxy of PAR available 5 mm deep in the cell suspension. It is in non-diluted, 100% cultures for all wavelengths more than 40% of the incident light. The $T_{h,\lambda,susp}$ spectra are affected dominantly by light absorption as the integrating sphere detects most of the forward scattered light and the backward scattering is assumed to be small. This is indicated by values of $T_{h,\lambda,susp}$ that approach more than 85% in the near infrared range in Fig. 1, right panel. In contrast, the $T_{n,\lambda,susp}$ spectra are affected by both light absorption and scattering because a high fraction of the scattered light is not detected by the low acceptance angle of the normal-normal detector.

Thus, the $T_{h,\lambda,susp}$ spectra have higher magnitudes than related $T_{n,\lambda,susp}$ spectra. The difference illustrates well that the usually measured normal-normal spectra are a poor proxy for light available 5 mm deep in algal photobioreactor. For example, $T_{n,\lambda,susp} \approx 0.3$ (Fig. 1, left panel) or optical density $D_{n,\lambda,susp} \approx 0.5$ (Fig. S3) cannot be interpreted as saying that only 30% of incident light is available for photosynthesis 5 mm deep in the photobioreactor.

The $T_{n,\lambda,susp}$ and $T_{h,\lambda,susp}$ spectra that are shown in Fig. 1 can be transformed as described in Materials and methods into the absorption and scattering coefficients, κ_λ and σ_λ that are presented in Fig. 2.

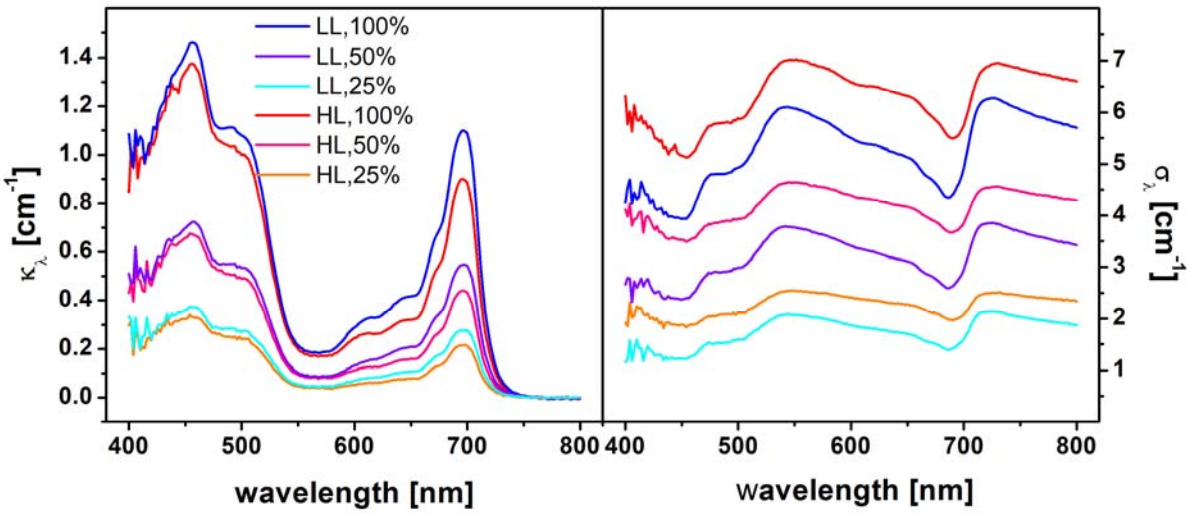

Figure 2. Spectra of absorption and scattering coefficients, κ_λ and σ_λ, respectively, of the LL and HL acclimated algal cells for the three different algal suspension dilutions.

The spectra show that the scattering coefficients, σ_λ, are 4–5 times higher than the corresponding absorbance coefficients, κ_λ. Thus, light is attenuated in algal suspension mostly by light scattering (see also Bricaud et al. 1983, Davies-Colley et al. 1986). It is noteworthy that the dips in the light scattering spectra appear at about same wavelengths as the peaks in the absorption spectra, as already described elsewhere (Bricaud and Morel 1986, Heng and Pilon 2014, Pilon and Kandilian 2016), a spectral feature that is attributed to the resonance behavior of scattering as represented by the real part of the complex index of refraction and absorption

represented by the imaginary part of the complex index of refraction. This resonance of scattering is particularly strong when absorption shows strong peaks.

The absorption and scattering coefficients are roughly proportional to culture density and thus characterize primarily cell culture rather than properties of the individual algal cells. The dependence of scattering and absorption on cell culture density can be reduced by normalization to dry weight, an operation that transforms coefficients κ_λ and σ_λ into cross-sections $S_{dw,\lambda}$ and $A_{dw,\lambda}$ that are shown in Fig. 3.

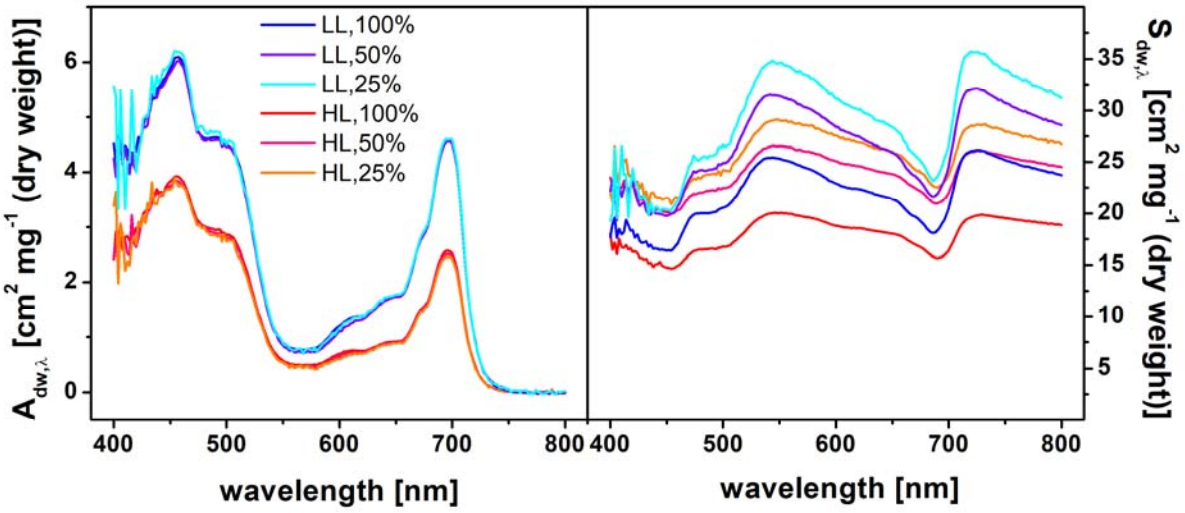

Figure 3. Spectra of absorption and scattering cross-sections normalized to dry algal cell weight, ($A_{dw,\lambda}$), and ($S_{dw,\lambda}$), respectively, of the LL- and HL-acclimated algal cells for the three different algal suspension dilutions.

The normalization to dry weight in the absorption cross-section $A_{dw,\lambda}$ largely eliminated differences between 100, 50 and 25% HL culture densities as well as between 100, 50 and 25% LL culture densities, indicating nearly linear relationship between the absorbance coefficient κ_λ and culture dry weight density. This means that the cells were not mutually shading each other even with 100% density.

Large differences were found however between absorption of LL and HL grown cells. The absorption cross-section $A_{dw,\lambda}$ in the LL *C. vulgaris* cells was significantly, ca. 1.55 times at 436 nm and ca. 1.85 times at 680 nm larger than in the HL cells (Fig. 3, left panel). The

difference can be interpreted as documenting stronger absorption by LL cells than by the HL cells, both on the dry-weight basis. A very similar qualitative and even quantitative changes were reported by de Mooij et al. (2017). Such results are expected, since cells grown in the LL-conditions must have a higher light-harvesting antennae to collect sufficient light energy necessary for photosynthetic function. This qualitatively corresponds to the ratio between chl and dry weight amounts which was 1.6·% (w/w) in LL cells and 1.2·% (w/w) in HL cells (Table 1) and, thus, the LL cells contained ca. 1.6 / 1.2 ≈ 1.3 times more chl in the same dry weight. The LL cells containing per dry weight 1.3 times more chl than the HL cells cannot, however, explain the entire difference in $A_{dw,\lambda}$ which was 1.55 times at 436 nm and ca. 1.85 times at 680 nm. Indeed, Fig. 4, left panel shows that the difference between LL and HL cells persisted even with the absorption cross-section $A_{chlw,\lambda}$, which was normalized directly to the chl content rather than to dry weight.

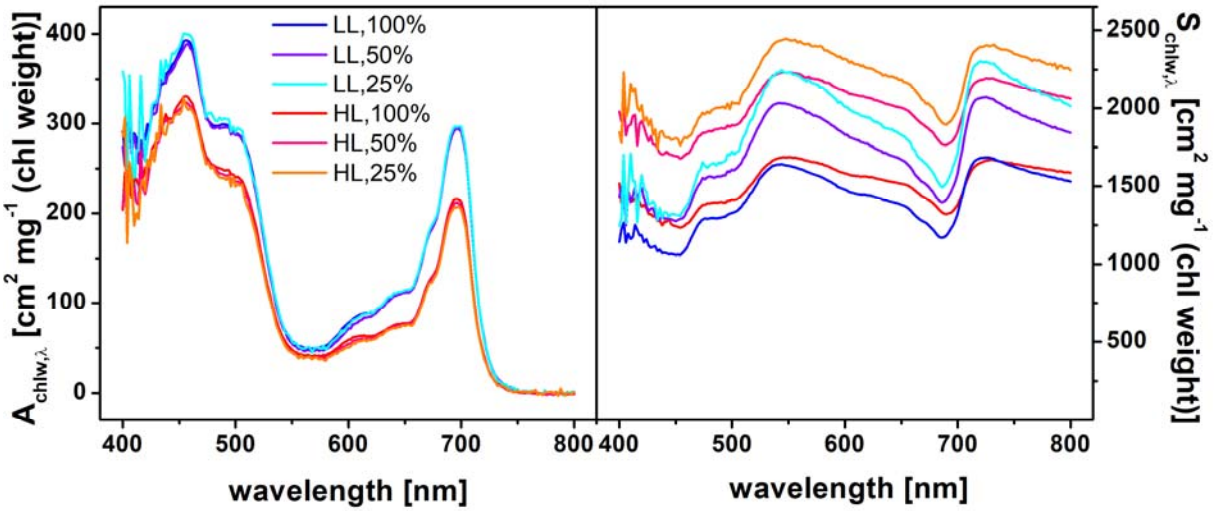

Figure 4. Spectra of absorption and scattering cross-sections normalized to chl (*a* + *b*) content in dry cell weight, $A_{chlw,\lambda}$ and $S_{chlw,\lambda}$, respectively, of the LL- and HL-acclimated algal cells for the three different algal suspension dilutions.

The difference in $A_{chlw,\lambda}$ between the LL and HL cells remained distinct in spite of the normalization to cell chl content indicating that the pigment molecules were not only more abundant in LL cells but also organized so that absorption of photons per pigment molecule

was more efficient than in HL cells. The differences are due to spatial inhomogeneity of pigments and beam path lengths (Nauš et al. 2018), which cause the sieve and detour effects (Duysens 1956, Das et al. 1967, Kirk and Goodchild 1972).

The scattering cross-section $S_{dw,\lambda}$ obtained by normalization to dry weight (Fig. 3, right panel) was dependent on culture density much less than the non-normalized scattering coefficient σ_λ (Fig. 2, right panel). Nevertheless, the residual differences in $S_{dw,\lambda}$ for 100, 50, and 25% suspension densities were higher than for the corresponding absorption cross-sections $A_{dw,\lambda}$ (Fig. 3), which can be explained by larger amplitude of scattering compared to absorption. Thus, stronger non-linearity in $S_{dw,\lambda}$ than in $A_{dw,\lambda}$ is to be expected. Convergence of $S_{dw,\lambda}$ curves for different suspension densities is expected if single scatter event occurs during the light beam pathway in the sample (Berberoglu et al. 2007, 2008). We obtained the results, even if the culture density of our cells (0.24 – 0.35 g(dw) L^{-1}; Table 1) was similar or even lower then density of cyanobacterium *Anabaena cylindrica* cells (0.202 – 0.431 g L^{-1}) used in Heng et al. (2014) or of *C. vulgaris* cells (0.560 g L^{-1}) used in in Kandilian et al. (2016a), where the curve convergence was obtained. Thus, we conclude that the IPPAS-C1 cells scatter light more than other cells, and more than single scatter event occurred during the light beam pathway in our sample suspensions. Further, the differences between the scattering by the HL and LL cells (compare, e.g., the 25% curves for HL and LL in Fig. 3 in the right panel) were relatively lower than the respective HL *vs*. LL differences in the absorption (compare, e.g., 25% curves for HL and LL in Fig. 3 in the left panel). This finding demonstrates that the internal organization of the cells that is decisive for scattering is less sensitive to HL and LL treatment than the cell pigment content that controls absorption.

Interestingly, on the dry-weight basis, the cells acclimated to LL scatter light more than the cells acclimated to HL (Fig. 3, right panel). Using the Lorenz-Mie theory (e.g., Kandilian et al., 2016a) and assuming the same average index of refraction of the LL and HL cells, one may

tentatively attribute the higher scattering in LL cells to their cell size that is smaller than in HL cells (Fig. S1, Supplementary materials). This does not exclude other potential effects such as different organization of cellular organelles and membrane systems, which might be different in the LL and HL cells, and which also influences scattering properties of phytoplankton cells (Witkowski et al. 1993, 1994, 1998).

Figure 4 shows in its right panel also the scattering cross-section $S_{chlw,\lambda}$ obtained by normalization of σ_λ to chl content. By comparison to the scattering coefficient σ_λ, (Fig. 2, right panel), the differences in $S_{chlw,\lambda}$ between the HL and LL acclimated cells are smaller (Fig. 4, right panel). Nevertheless, the scattering is not directly caused by interactions of photons with chl molecules and, thus, normalization to chl content has no direct and simple interpretation.

Generally, the absorption and scattering spectra of *C. vulgaris* IPPAS C1 presented in Figs. 2, 3, and 4 are qualitatively similar to the spectra of *C. sp*. (Berberoglu et al. 2009) and *C. vulgaris* (Kandilian et al. 2016a). Kandilian et al. (2016b) published $A_{dw,\lambda}$ and $S_{dw,\lambda}$ spectra of *C. vulgaris* grown in 200 μmol (photons) m^{-2} s^{-1}, conditions almost identical to the LL in this study. Remarkable is the strong scattering that Pilon and Kandilian (2016) attributed to the relatively thick cell wall of *Chlorella* species, which may strongly refract light. In our study, we observed that scattering cross-sections of *C. vulgaris* IPPAS C1 were also dramatically larger than absorption cross sections. To quantify and compare effects of scattering and of absorption in a simple parameter, we used the ratio of scattering at 750 nm where absorption is negligible to the absorption red peak (676 nm) (S750/A676). In the spectra measured with microalgae *Botryococcus branuii*, *Chlorella* sp., *Chlorococcum litorale* and *Chlamydomonas reinhardtii* by Berberoglu et al. (2009) and by Kandilian et al. (2016a) the S750/A676 ratios were found within the range of 6.1 – 8.0. In the much smaller cells of cyanobacteria *Anabaena cylindrica* and *Synechocystis* sp. (Heng et al. 2014, 2016) the S750/A676 ratios were only slightly lower (6.9 – 7.2). The spectra of *Chlorella vulgaris* grown at 500 or 200 μmol (photons) m^{-2} s^{-1} show

the S750/A676 ratios of 7.0 and 7.5, respectively (Kandilian et al. 2016a, 2016b). In our study of *C. vulgaris* IPPAS C1 the ratio was found 5.4–7.1 in the LL cells and 7.5–11.2 in the HL-acclimated cells. Our results for the LL-acclimated cells agree well with the results of Kandilian et al. (2016b) obtained for algae grown in a very similar light environment. In contrast to this, our spectra of HL-acclimated cells exhibit significantly higher S750/A676 ratios than in any of the other organisms. Based on that we suggest that the increased light scattering by the HL-acclimated IPPAS-C1 cells might be responsible for increased HL resilience reported in literature for these cells (Treves et al. 2013, 2016). However, more research on this topic is required.

If considered as proxies for culture density or chl density, the results presented here show clearly that the scattering and absorption coefficients ought to be calibrated for each particular irradiance to which the algae are acclimated. The quantification of the differences between HL and LL cells shows what experimental systematic error one should expect when using a single OD/dw calibration in batch cultures, in which the exponential phase starts with a very dilute culture (effective HL) and ends with stationary highly dense cultures (effectively LL). In addition the results show that separating absorption coefficient by an integrating sphere is the way to increase the range of linearity of the optical proxy. The main conclusion of this study is that optical properties of this fast-growing, high-light resilient *C. vulgaris* IPPAS C1 are very flexible.

3.2 Optical properties of Chlorella cultures during algal cell cycle

Algal cells undergo a cell cycle with mother cells dividing into much smaller and morphologically distinct daughter cells and with their subsequent growth. Changes in composition and amount of proteins, polysaccharides and amino, keto and fatty acids, which occur during the *Chlorella* cell cycle were investigated and described in detail (Kanazawa 1964, Otsuka and Morimura 1966, Kanazawa et al. 1967, Kanazawa and Kanazawa 1968, Takeda and

Hirokawa 1978). Considering changes in size and structure of the cells, it is plausible to expect that absorption and scattering properties of individual cells will substantially change during the cell cycle. Video in Supplementary materials illustrates these dynamic changes (Fig. S5).

It is frequently assumed that algal cultures in biotechnological applications are approximately asynchronous and, thus, that the optical properties represent a mean value making, for example, optical density a good proxy for culture dry weight. This may be the case for asynchronous cultures that are grown under constant, e.g., turbidostat conditions such as represented in Fig. S1 (Supplementary materials). The quality and stability of such optical proxy needs however to be verified for more real-life conditions because light-dark diurnal changes, dilutions, changes in temperature, and many other factors or interventions may lead to culture synchronization that will in turn modulate absorption and scattering properties of algal cells by processes illustrated in Fig. S5 of Supplementary materials.

To investigate impact of cell cycle dynamics on optical properties of *C. vulgaris* IPPAS C1, the culture was synchronized by 3 consecutive diurnal cycles with 14 hours dark and 10 hours of 1760 μmol (photons) m^{-2} s^{-1}. The light phase corresponded to the HL treatment in the experiments described above. Figure S6, left panel in Supplementary materials shows that the culture was characterized by a narrow size distribution with a diameter maximum around 2.5 μm which corresponds to a cell volume of ca. 8.2 μm^3. The cell diameter representing most of the growing cells at the end of the light period was ca. 3.6 μm that corresponded to ca. 24.4 μm^3. The mother cell distribution was, unlike the cells at the beginning of the light period, rather broad indicating that mother cells could contain 2, 4, or even 8 daughter cells (division into 8 daughter cells is illustrated in the Fig. S5 video in the Supplementary materials). The diameters of the mother cells of a volume corresponding to two, four, and eight daughter cells (ca. 16.4, 32.8, and 65.6 μm^3, respectively) would be roughly 3.2, 4.0 and 5.0 μm, respectively,

all present in the distributions of cell diameters at the end of the light phase (Fig. S6, left panel) and at the beginning of the dark phase of the cell cycle (Fig. S6, right panel).

The transmittance spectra $T_{n,\lambda,susp}$ measured in conventional spectrophotometer and the spectra $T_{h,\lambda,susp}$ measured with integrating sphere during the cell cycle are presented in Fig. 5. The corresponding spectra of $T_{n,\lambda,cells}$ and $T_{h,\lambda,cells}$ (see Material and methods), as well as absorbance spectra of $D_{n,\lambda,susp}$ and $D_{n,\lambda,cells}$ during the cell cycle are shown in Figs. S7 – S9 (Supplementary materials). Figure 5 shows that transmittance measured both without ($T_{n,\lambda,susp}$) and with an integrating sphere ($T_{h,\lambda,susp}$) decrease as the cells grow during the light phase, a change that is largely reversed by the cell division early in the dark phase of the cell cycle.

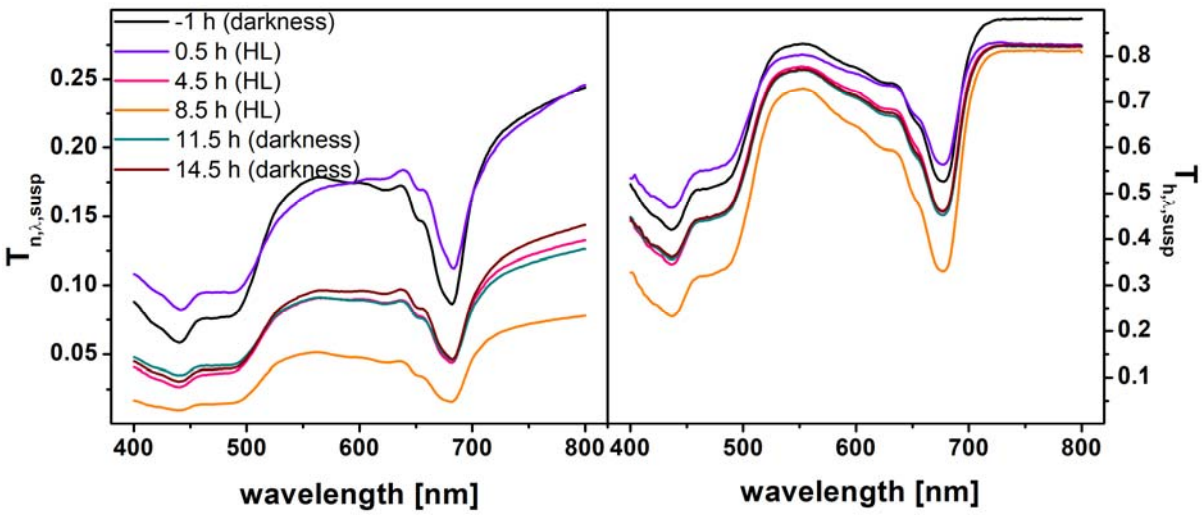

Figure 5. The normal-normal and normal-hemispherical transmittance spectra, $T_{n,\lambda,susp}$ and $T_{h,\lambda,susp}$, respectively, of algal cell suspension measured during the cell cycle. The HL was switched on (time 0) for 10 hours and the cells were kept in darkness before and after the HL. The spectra show transmittance at 5 mm (see Material and methods).

The transmittance spectra in Fig. 5 combine effects of absorption as well as of scattering. These are separated in Fig. 6 that shows the absorption and light scattering coefficients, κ_λ and σ_λ, respectively. The figure shows that spectra of both scattering σ_λ and absorption κ_λ are changing during the cell cycle and that σ_λ is again several times higher than κ_λ.

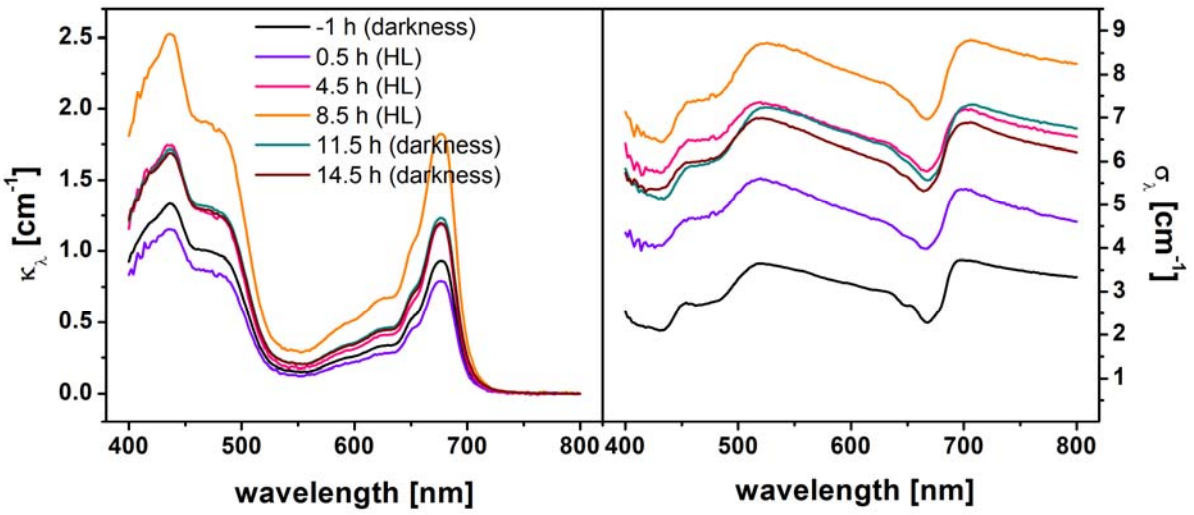

Figure 6. Spectra of absorption and scattering coefficients, κ_λ and σ_λ, respectively, obtained during cell cycle. The HL was switched on (time 0) for 10 hours and the cells were kept in darkness before and after the HL.

Figure 7 shows the spectra of absorption and scattering cross-sections $A_{dw,\lambda}$ and $S_{dw,\lambda}$ that are normalized to the dry weight of the algal suspension.

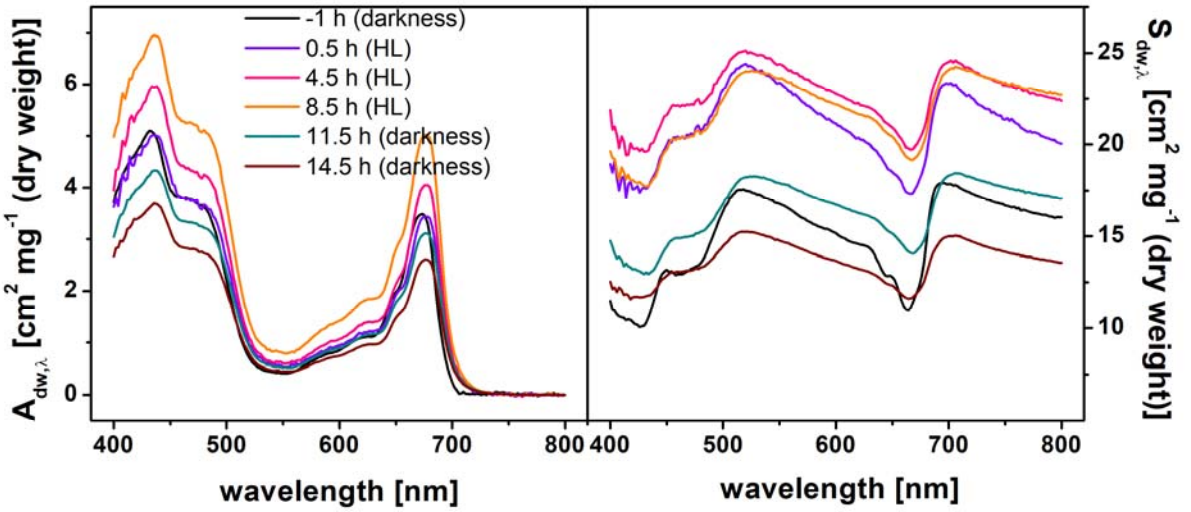

Figure 7. Spectra of absorption and scattering cross-sections normalized to dry algal weight, $A_{dw,\lambda}$ and $S_{dw,\lambda}$, respectively, during cell cycle. The HL was switched on (time 0) for 10 hours and the cells were kept in darkness before and after the HL exposure.

The normalization reduces the differences between the cross-sections $A_{dw,\lambda}$ and $S_{dw,\lambda}$ (Fig. 7) relative to the coefficients κ_λ and σ_λ (Fig. 6) but the increase of absorbance cross-sections $A_{dw,\lambda}$ during the light phase of the cell cycle remains significant. The most dramatic reversal in this

trend is observed between the end on the light phase (8.5^{th} h) and beginning of the dark phase (11.5^{th} h) when the cells prepare for cell division. A dramatic decrease of photosynthetic activity is also observed during this process in Chlorella (Sorokin 1957, Nara et al. 1989) as well as in other algae (Kaftan et al. 1999). The scattering cross-section $S_{dw,\lambda}$ significantly increased when the cells were transferred from the initial dark-adapted state to the light phase of the cell cycle but $S_{dw,\lambda}$ changed only little during growing of the cells in the light phase (Fig. 7, right panel). Subsequently, during the division of the cells in darkness, the $S_{dw,\lambda}$ significantly decreased to or even lower values as observed in the initial dark adapted state. Interestingly, the above phenomena can be seen even by a bare eye, which can read a text through a cuvette with suspension of dividing cells whereas the text is largely blurred by scattering with growing cells (not shown). The increased $S_{dw,\lambda}$ during the growth of the cell in the light phase (Fig. 7, right panel) is, however, not compatible with increased average cell diameter in the light phase (Fig. S4, left panel). Thus, the increased $S_{dw,\lambda}$ is probably caused by internal cell structures and interfaces, which change their spatial parameters (e.g., starch grains, grana thylakoids, chloroplast walls, etc.) during the cell growth (see below). A role of internal cell structures and interfaces on scattering properties of phytoplankton cells has already been reported (Witkowski et al. 1993, 1994, 1998).

The spectra of the absorption and scattering coefficients (Fig. 6) can be also normalized to chl content yielding absorption and scattering cross sections $A_{chlw,\lambda}$ and $S_{chlw,\lambda}$ that are shown in Fig. 8. The absorption cross section $A_{chlw,\lambda}$ is varying only slightly during the cell cycle indicating that most of the absorption-related changes in transmittance during the cell cycle (Fig. 5) can be attributed to changing chl content. Interestingly, the normalization to chl reduced largely also the variability of the scattering cross section $S_{chlw,\lambda}$ (Fig. 8, right panel).

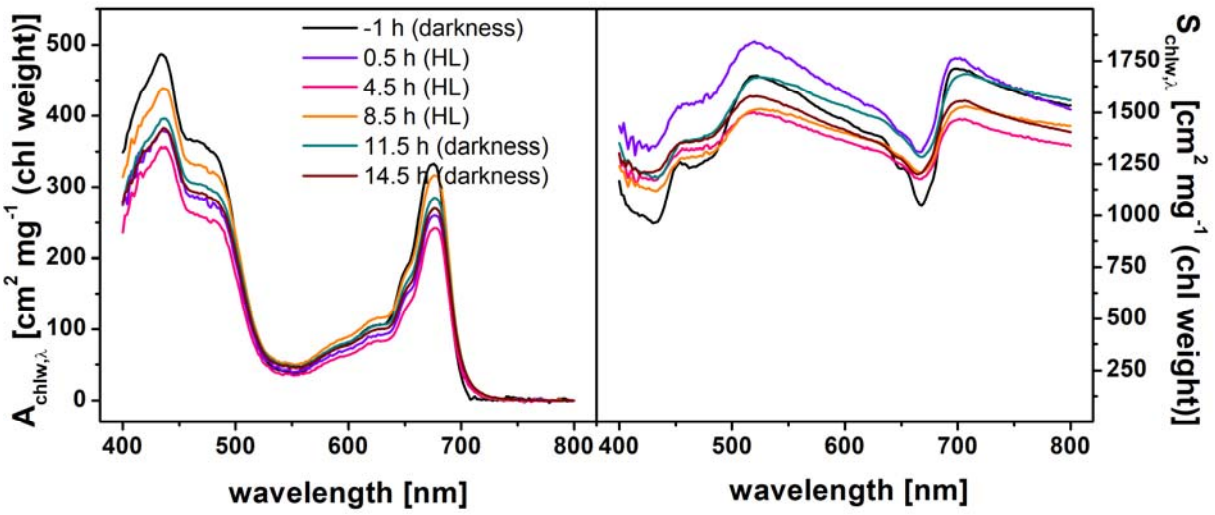

Figure 8. Spectra of absorption and scattering cross-sections normalized to dry cell weight chl ($a + b$) content, ($A_{chlw,\lambda}$), and ($S_{chlw,\lambda}$), respectively, during cell cycle. The HL was switched on (time 0) for 10 hours and the cells were kept in darkness before and after the HL exposure.

As far as we know, five studies measured/calculated spectra of absorption and scattering coefficients/cross sections of photosynthetic aquatic organisms during their cell culture growth; Heng et al. (2014) measured the optical spectra during growth (6–14 days) of cyanobacterium *Anabaena cylindrica*, Heng and Pilon (2014) measured the spectra during growth (up to 308 hours) of marine algae *Nannochloropsis oculata*, Zhao et al. (2018) measured the spectra during growth (up to 435 hours) of microalgae species *Chlorella vulgaris*, *Chlorella pyrenoidosa* and *Chlorella protothecoides*, and Ma et al. (2018) measured the spectra during growth (up to 617 hours) of filamentous cyanobacterium *Spirulina platensis*. Further, Ma et al. (2019) calculated the optical spectra by means of Lorenz-Mie theory based on experimental data of *Chlorella vulgaris* growth during 15 days (Dewan et al. 2012). However, growth of batch cultures was explored in all five studies. Thus, the results obtained in the five studies cannot be compared with our results upon one growth cycle of synchronous cell culture. To somehow simply characterize dynamics of optical properties during the cell cycle, we evaluated changes of scattering cross-sections at 750 nm ($S_{chlw,750}$, $S_{dw,750}$, absorption is negligible at this wavelength) and absorption cross-sections at 676 nm ($A_{chlw,750}$, $A_{dw,750}$, red absorption peak) during the cell

cycle relative the respective cross section value in the beginning of cell cycle measurement, see Fig. S10 (Supplementary materials). While the cross-sections per chl content varied up to 30% of the initial value, mostly decreasing, changes in the cross-sections per dry weight first increased by about 40 – 50% and then decreased by about 10 – 25% below the initial value.

Witkowski et al. (1993) studied cell cycle (up to 10 days) of a slowly growing *Chlorella vulgaris* cells, however, they have not measured the optical spectra directly but they used the methods of integral and dynamic light scattering. They have found that particles, which might be cell organelles, with a diameter of about 0.3 μm contribute to the light scattering during the cell cycle. Subsequent studies by Witkowski et al. (1994, 1998) confirmed a role of intracellular structures in the light scattering of *Chlorella* and other phytoplankton cells. In connection to that, light scattering caused by cell organelles has been successfully considered in modelling of optical properties of leaves (Berdnik and Mukhamedyarov 2001, Krekov et al. 2009, Watté et al. 2015, Ho et al. 2016).

3.3 Ultrastructure of Chlorella cells during the algal cell cycle

The transmission electron microscopy images of *C. vulgaris* IPPAS C1 cells taken during selected time-points of the cell cycle are shown in Fig. 9. The key ultrastructural features of *C. vulgaris* IPPAS C1 acclimation to HL included an increase in the size of cell and chloroplast, accumulation of starch grains (both inter-thylakoid and those of the pyrenoid sheath) decline in the thylakoid stacking, increase in the rubisco-containing matrix of the pyrenoid and expansion of the periplasmic space. Generally, these features are consistent with those previously documented in microalgae (Berner et al. 1989, Berner and Sukenik 1998). On the other hand, formation of autospores within the cell wall of the mother cell during cell division phase in the darkness is characterized by a wide periplasmic space as well as the space between the autospores (Fig. 9c).

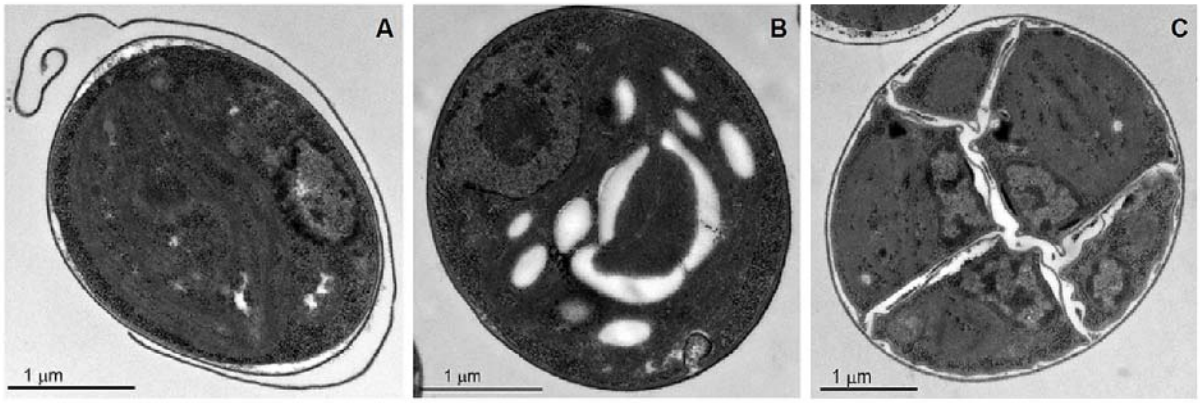

Figure 9. The ultrastructure of *Chlorella vulgaris* IPPAS C-1 cells kept in darkness (A, -1 h in related figures), in the HL illumination (B, 8.5 h) and in subsequent darkness (C, 11.5 h). The white flecks in B are starch grains whereas nascent autospores within the cell wall of the mother cell are shown in C. Also note a wide periplasmic space as well as the space between the autospores in C.

For finding a possible correlation of the ultrastructural changes of the cells during their cell cycle with changes in the absorption and scattering cross-section spectra during the cell cycle, we quantified in detail the ultrastructural organization of IPPAS C-1 cells sampled during the cell cycle. These results are shown in Fig. 10. During the light period, the cell area increased before the onset of the dark period (Fig. 10A, black symbols). The changes in the protoplast area followed a similar trend (Fig. 10A, red symbols) suggesting minor variation in the cell wall *per se* during the cell cycle. Indeed, direct measurements of the cell wall thickness did not show sizeable changes (Fig. 10B, red symbols). On the contrary, combined area of cell wall and periplasmic space changed dramatically in the progress of cell cycle (Fig. 10B, black symbols). The most spectacular size of the periplasmic space constituting a clearly distinguishable interphase (1.69 ± 0.14 µm; Fig. 9C), potentially contributing to light scattering, was typical of the dividing cells. The trend of changes in the chloroplast area (Fig. 10C, black symbols) was similar to that of the cell area (Fig. 10A, black symbols) resulting in a modest variation in the proportion of chloroplast in the total area of the protoplast (Fig. 10C, red symbols). Another conspicuous change in the cell organization was constituted by the changes in total area of

starch grains (Fig. 10D, black symbols) and number of starch grains (Fig. 10D, red symbols), which apparently determines the dynamics of the cell size. Notably, the cell division, which started soon after beginning of the dark period (at time 10.5 h) and continued afterword, is clearly visible in the trends of changes in the size of the cells and subcellular structures.

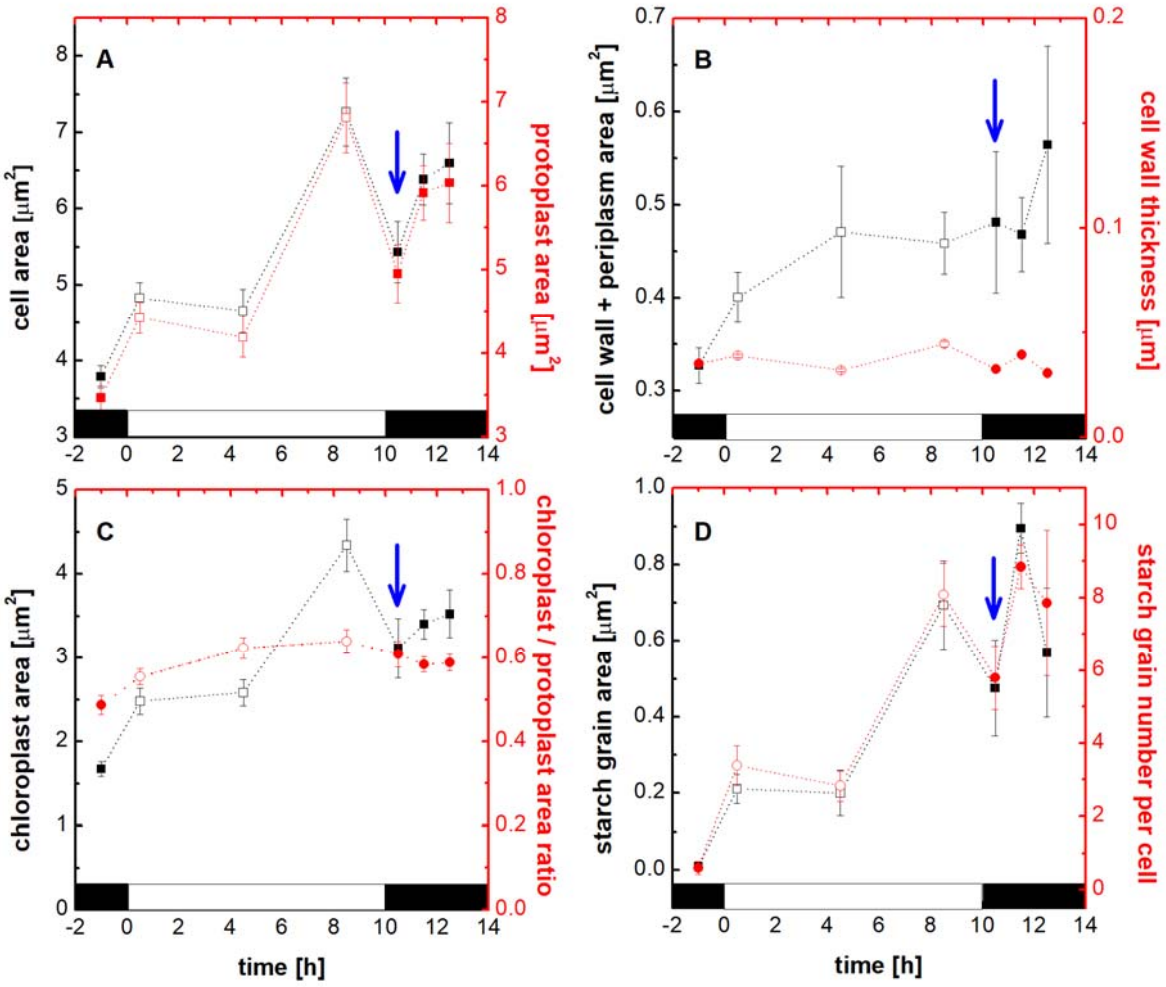

Figure 10. The time-course of changes in mean (A) cell and protoplast area, (B) area of cell wall with periplasmic space and cell wall thickness, (C) absolute area of the chloroplast and its proportion in the protoplast area, and (D) total starch grains area and number of starch grains per cell during cell cycle in the *C. vulgaris* IPPAS C-1. The vertical arrow indicates the approximate moment of beginning of cell division. Error bars indicate standard error (n=32). Black and white bars show the dark and light phases of the photoperiod, respectively. Dotted lines are used to better distinguish data of the same type.

To reveal relationships between the observed changes in cell structure progressing through the cell cycle and their optical properties, we calculated correlation coefficients for ultramicromorphometric parameters and corresponding values of absorption or scattering cross-

sections per dry weight (Fig. 11). Spectra of the correlation coefficients between the parameters and $A_{dw,\lambda}$ (Fig. 11A, C) are very similar in shape except of one spectrum. The shapes are characterized by decline of correlation coefficient at wavelengths of strong chl absorption. This can be explained by the fact that during growing of the cells, not only amount of light-absorbing chl molecules is changed, but also morphology of corresponding cell structures, i.e., packing of chls in chloroplasts. This process is accompanied by changes in heterogeneity of chl concentration, which was shown to lead to nonlinearity of light absorption (Baránková et al. 2016, Nauš et al. 2018). The nonlinearity might be the reason of the decline of the correlation coefficient. This is evident not only in spectra of correlation coefficient between $A_{dw,\lambda}$ and parameters related to chl content (chloroplast area, chloroplast area relative to protoplast area (Fig. 11C), cell area (Fig. 11A)) but also in spectra of correlation coefficient between $A_{dw,\lambda}$ and area of cell wall and periplasmic space (Fig. 11A), and area of starch grains (Fig. 11C). The latter is not surprising since changes in the starch grain parameters follow the same trends as changes in the chl content parameters (Fig. 10). On the other hand, correlation between thickens of cell wall and $A_{dw,\lambda}$ shows only a small dependence on wavelength (Fig. 11A); it might reflect the fact that cell wall interfaces scatter light before it reaches chls, and thus remaining light entering cell is very little attenuated by the pigment absorption.

Also spectra of the correlation coefficients between the ultramicromorphometric parameters and $S_{dw,\lambda}$ (Fig. 11B, D) are very similar in shape except of one spectrum. The shape resembles shape of spectrum reciprocal to sum of the absorption and scattering cross section spectra (data not shown). This indicates that the correlations are nonlinear function not only of light scattering but also of light absorption. Again, only spectrum of the correlation coefficient between thickness of cell wall and $S_{dw,\lambda}$ shows rather flat spectrum (Fig. 11B), indicating that it is not affected by light absorption.

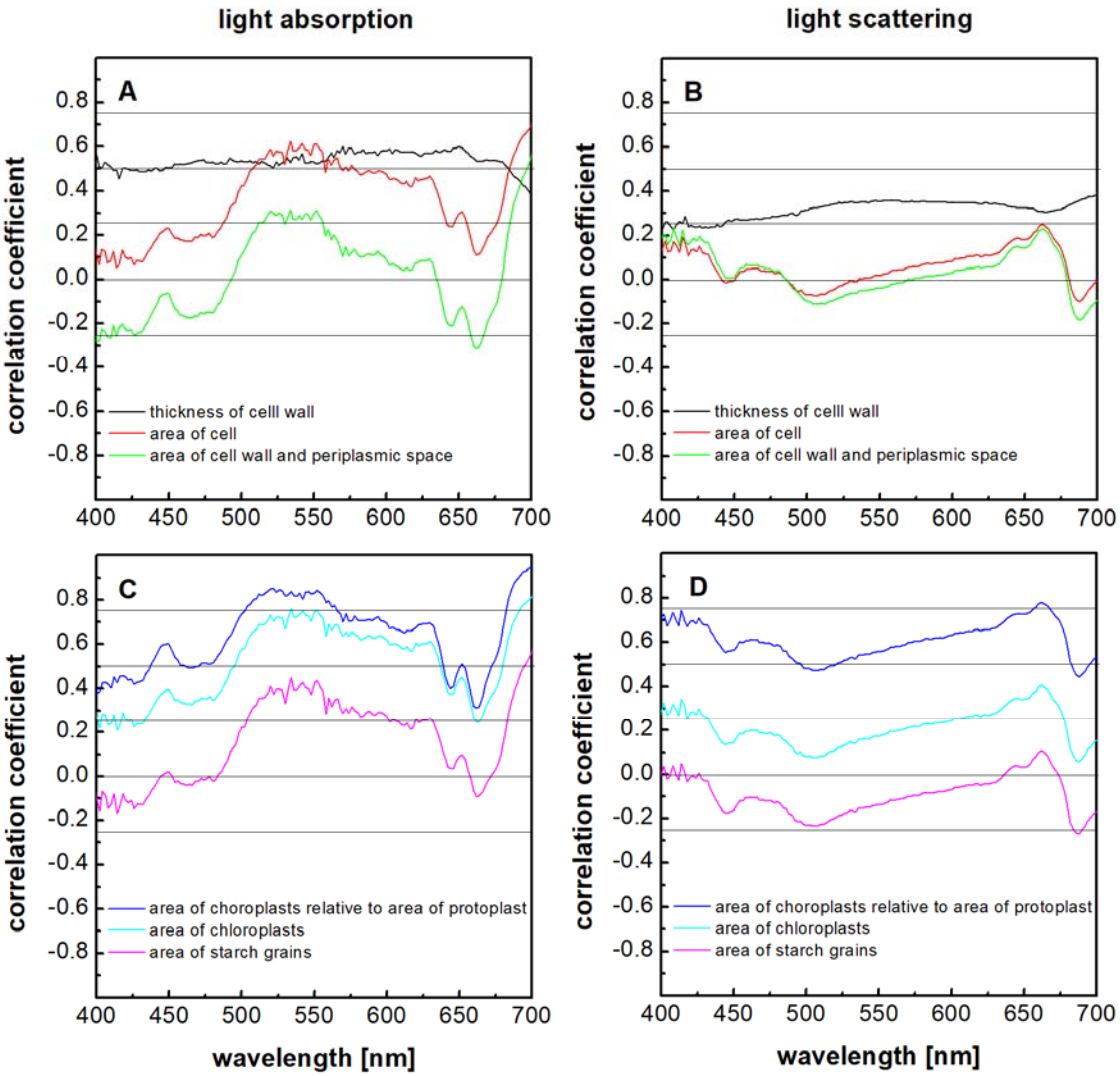

Figure 11. Spectra of Pearson correlation coefficient calculated for the relationships between changes in cell organization and optical properties of the *C. vulgaris* IPPAS C-1 cells in the course of cell cycle. The correlation between cell and cell wall parameters (A, B) as well as chloroplast and starch grain parameters (C, D) and absorption (A, C) or scattering (B, D) cross-section per dry weight ($A_{dw,\lambda}$ and $S_{dw,\lambda}$) are shown.

For numerical evaluation of the correlations, we use following key: $-0.25 < r < 0.25$, no correlation; $0.25 < r < 0.5$ ($-0.5 < r < -0.25$), weak positive (negative) correlation; $0.5 < r < 0.75$ ($-0.75 < r < -0.5$), moderate positive (negative) correlation; $0.75 < r$ ($-0.75 > r$), strong positive (negative) correlation. In the blue and red chl absorption regions, no correlation was found between $A_{dw,\lambda}$ and area of starch grains (Fig. 11C), and area of cells, and area of cell wall and periplasmic space (Fig. 11A). Weak correlations between $A_{dw,\lambda}$ and area of chloroplasts and

area of chloroplasts relative to protoplast (Fig. 11C) was found in the red and blue regions. Surprisingly, the highest correlation in the blue and red absorption region was found between $A_{dw,\lambda}$ and thickness of cell wall. In the green and near infra-red regions of the spectrum, where light is not absorbed but rather scattered, no correlation was found between $S_{dw,\lambda}$ and area of cell, and area of cell wall and periplasmic space (Fig. 11B), and between $S_{dw,\lambda}$ and area of chloroplasts, and area of starch grains (Fig. 11D). Weak correlation between $S_{dw,\lambda}$ and thickness of cell wall was found in the green and infra-red regions (Fig. 11B) and the highest correlation in the spectral regions was found between $S_{dw,\lambda}$ and area of chloroplasts relative to area of protoplast (Fig. 11D). The area of chloroplasts relative to area of protoplast reflects a relative amount of interfaces between chloroplast membrane (outer, inner) and its surrounding, the interfaces being source of light scattering by light refraction. A crucial role of cell organelles in light scattering has already been implicitly inferred from measurement of optical properties of phytoplankton cells (Witkowski et al. 1993, 1994, 1998) and has also been explicitly assumed in modelling of optical properties of leaves (Berdnik and Mukhamedyarov 2001, Krekov et al. 2009, Watté et al. 2015, Ho et al. 2016). However, we have shown that the correlations do exist on the basic of direct measurement of the optical properties and ultramicromorphometric parameters of the cells during their cell cycle.

4. Conclusion

We have shown that the asynchronous cultures of *Chlorella vulgaris* IPPAS C1 cells acclimated to high-light and low-light conditions have different optical properties. The comparative analysis of the changes in ultrastructure and optical properties of the studied microalgae revealed that the high light acclimation, as well as progressing of the cell cycle results in dramatic changes in light scattering structures within the cell. On the contrary, alteration of qualitative and quantitative composition of pigment apparatus were modest in comparison with changes in light scattering capacity of the *C. vulgaris* cells under our experimental conditions.

Collectively, the findings in this work suggest that the acclimation of IPPAS-C1 to a relatively short exposure of moderately high light is carried out largely by modulation of the scattering cross-section of the cell rather than by altering their content and composition. A vast increase of light scattering of the cells in preparation to the cytokinesis might play a role in photoprotection of the cell in this period when its photosynthetic activity is depressed but chl content remains as high.

Authors´ contributions

L.N. D.L. and A.S. conceptualized the study. B.B. performed the optical measurements and O.G. with O.B. performed ultramicromorphometric measurements. B.B, D.L., L.N., J.N., and G.H. evaluated the optical data and O.G., O. B., and A.S. evaluated the ultramicromorphometric data. B.B., D.L., L.N., and A.S. wrote parts of the first manuscript draft. J.N. and G.H. substantially contributed to a revised version of the manuscript.

Statement of informed consent, human/animal rights

No conflicts, informed consent, or human or animal rights are applicable to this study.

Acknowledgement

BB, DL, and JN were supported by the grant No. LO1204 (Sustainable Development of Research in the Centre of the Region Haná) from the National Program of Sustainability I, Ministry of Education, Youth and Sports, Czech Republic and DL was also supported from ERDF project “Plants as a tool for sustainable global development” (no. CZ.02.1.01/0.0/0.0/16_019/0000827). AS acknowledges financial support of the Science Foundation for Basic Research (grant 18-29-25050) and a partial financial support of the Moscow State University Grant for Leading Scientific Schools "Depository of the Living Systems" in frame of the MSU Development Program. The research of GH and LN in Forschungszentrum Julich, Germany, was financially supported by the BioSC AlgalFertilizer project funded by the Ministry of Innovation, Science and Research of the German State of North Rhine-Westphalia. Responsibility for the content of this publication remains with the authors. The ultrastructure studies were carried out at the User Facilities Center of M.V. Lomonosov Moscow State University.

References

Aiba S. (1982) Growth kinetics of photosynthetic microorganisms. Microbial Reactions 23, 85–156

Baránková B., Lazár D., Nauš J. (2016) Analysis of the effect of chloroplast arrangement on optical properties of green tobacco leaves. Remote Sensing of Environment 174, 181–196

Berberoglu H., Gomez P.S., Pilon L. (2009) Radiation characteristics of *Botryococcus braunii*, *Chlorococcum littorale*, and *Chlorella sp.* used for CO_2 fixation and biofuel production. Journal of Quantitative Spectroscopy & Radiative Transfer 110, 1879–1893

Berberoglu H., Pilon L., Melis A. (2008) Radiation characteristics of *Chlamydomonas reinhardtii* CC125 and its truncated chlorophyll antenna transformants tla1, tlaX and tla1-CWD$^+$. International Journal of Hydrogen Energy 33, 6467–6483

Berberoglu H., Yin J., Pilon L. (2007) Light transfer in bubble sparged photobioreactors for H_2 production and CO_2 mitigation. International Journal of Hydrogen Energy 32, 2273–2285

Berdnik V.V., Mukhamedyarov R.D. (2001) Radiative transfer in plant leaves. Optics and Spectroscopy 90, 580–591

Berner T., Dubinsky Z., Wyman K., Falkowski P.G. (1989) Photoadaptation and the "package" effect in *Dunaliella tertiolecta* (Chlorophyceae). Journal of Phycology 25 70–78

Berner T., Sukenik A. (1998) Photoacclimation in photosynthetic microorganisms: an ultrastructural response. Israel Journal of Plant Sciences 46, 141–146

Bhowmik A., Pilon L. (2016) Can spherical eukaryotic microalgae cells be treated as optically homogeneous? Journal of the Optical Society of America A 33, 1495–1503

Böhm H. (1973) Das Chlorella-Testsystem (eine Übersicht). Wissenschaftliche Hefte der Pädagogischen Institut Köthen 2, 9–16

Bricaud A., Morel A. (1986) Light attenuation and scattering of phytoplanktonic cells: a theoretical modeling. Applied Optics 25, 571–580

Bricaud A., Morel A., Prieur L. (1983) Optical efficiency factors of some phytoplankters. Limnology and Oceanography 28, 816–832

Das M., Rabinowitch E., Szalay L., Papageorgiou G. (1967) The "sieve effect" in Chlorella suspensions. Journal of Physical Chemistry 71, 3543–3549

Dauchet J., Blanco S., Cornet J.-F., Fournier R. (2015) Calculation of the radiative properties of photosynthetic microorganisms. Journal of Quantitative Spectroscopy & Radiative Transfer 161, 60–84

Dewan A., Kim J., McLean R.H., Vanapalli S.A., Karm M.N. (2012) Growth kinetics of microalgae in microfluidic static droplet arrays. Biotechnology and Bioengineering 109, 2987–2996

Davies-Colley R.J. (1983) Optical properties and reflectance spectra of 3 shallow lakes obtained from a spectrophotometric study, New Zealand Journal of Marine and Freshwater Research, 17, 445–459

Davies-Colley R.J. Pridmore R.D., Hewitt J.E. (1986) Optical properties of some freshwater phytoplanktonic algae. Hydrobiologia 133, 165–178

de Mooij T., Nejad Z.R., van Buren L., Wijffels R.H., Janssen M. (2017) Effect of photoacclimation on microalgae mass culture productivity. Algal Research 22, 56–67

Douskova I., Doucha J., Livansky K., Machat J., Novak P., Umysova D., Zachleder V., Vitova M. (2009) Simultaneous flue gas bioremediation and reduction of microalgal biomass production costs. Applied Microbiology and Biotechnology 82, 79–185

Droop M. (1983) 25 years of algal growth kinetics. A personal view. Botanica Marina 26, 99–112

Duysens L.N.M. (1956) The flattening of the absorption spectrum of suspension as compared to that of solutions. Biochimica et Biophysica Acta 19, 1–12

Fuente D., Keller J., Conejero J.A., Rögner M. Rexroth S., Urchueguía J.F. (2017) Light distribution and spectral composition within cultures of micro-algae: Quantitative modelling of the light field in photobioreactors. Algal Research 23, 166–177

Fuente D., Lizama C., Urchueguía J.F., Conejero J.A., (2018) Estimation of the light field inside photosynthetic microorganism cultures through Mittag-Leffler functions at depleted light conditions. Journal of Quantitative Spectroscopy & Radiative Transfer 204, 23–26

Fukshansky L., Kazarinova N. (1980) Extension of the Kubelka-Munk theory if light propagation in intensely scattering materials to fluorescence media. Journal of the Optical Society of America 70, 1101–1111

Gaigalas A.K., He H.-J., Wang L. (2009) Measurement of absorption and scattering with an integrating sphere detector: application to microalgae. Journal of Research of the National Institute of Standards and Technology 114, 69–81

Ganapol B.F., Johnson L.F., Hammer P.D., Hlavka C.A., Peterson D.L. (1998) LEAFMOD: A new within-leaf radiative transfer model. Remote Sensing of Environment 63, 182–193

Gorelova O., Baulina O., Solovchenko A., Selyakh I., Chivkunova O., Semenova L., Scherbakov P., Burakova O., Lobakova E. (2015) Coordinated rearrangements of assimilatory and storage cell compartments in a nitrogen-starving symbiotic chlorophyte cultivated under high light. Archives of Microbiology 167, 181–195

Gorman D.S., Levine R.P. (1965) Cytochrome f and plastocyanin – their sequence in photosynthetic electron transport chain of *Chlamydomonas reinhardi*. Proceeding of the National Academy of Sciences of the United States of America 54, 1665–1669

Heng R.-L., Lee E., Pilon L. (2014) Radiation characteristics and optical properties of filamentous cyanobacterium *Anabaena cylindrica*. Journal of the Optical Society of America A 31, 836–845

Heng R.-L., Pilon L. (2014) Time-dependent radiation characteristics of *Nannochloropsis oculata* during batchculture. Journal of Quantitative Spectroscopy & Radiative Transfer 144, 154–163

Heng R.-L., Pilon L. (2016) Radiation characteristics and effective optical properties of dumbbell-shaped cyanobacterium *Synechocystis sp*. Journal of Quantitative Spectroscopy & Radiative Transfer 174, 65–78

Heng R.-L., Sy K.C., Pilon L. (2015) Absorption and scattering by bispheres, quadspheres, and circular rings of spheres and their equivalent coated spheres. Journal of the Optical Society of America A 32, 46–60

Henyey L.C., Greenstein J.L. (1941) Diffuse radiation in the galaxy. Astrophysical Journal 93, 70–83

Ho Q.T., Berghuijs H.N.C., Watté R., Verboven P., Herremans E., Yin X., Retta M.A., Aernouts B., Saeys W., Helfen L., Farquhar G.D., Struik P.C., Nicolaï B.M. (2016) Three-dimensional microscale modelling of CO_2 transport and light propagation in tomato leaves enlightens photosynthesis. Plant, Cell and Environment 39, 50–61

Huang J., Li Y., Wan M., Yan Y., Feng F., Qu X., Wang J., Shen G., Li W, Fan J., Wang W. (2014) Novel flat-plate photobioreactors for microalgae cultivation with special mixers to promote mixing along the light gradient. Bioresource Technology 159, 8–16

Kaftan D., Meszaros T., Whitmarsh D., Nedbal L. (1999) Characterization of photosystem II activity and heterogeneity during the cell cycle of the green alga *Scenedesmus quadricauda*. Plant Physiology 120, 433–442

Kanazawa T. (1964) Changes in amino acid composition of *Chlorella* cells during their life cycle. Plant and Cell Physiology 5, 333–354

Kanazawa T., Kanazawa K. (1968) Changes in composition patterns of basic proteins in *Chlorella* cells during their life cycle. Plant and Cell Physiology 9, 701–708

Kanazawa T., Kanazawa K., Nishimura T. (1967) Changes in contents of keto acids in *Chlorella* cells during their synchronized life cycle. Plant and Cell Physiology 8, 529–533

Kandilian R., Pruvost J., Artu A., Lemasson C., Legrand J., Pilon L. (2016a) Comparison of experimentally and theoretically determined radiation characteristics of photosynthetic microorganisms. Journal of Quantitative Spectroscopy & Radiative Transfer 175, 30–45

Kandilian R., Soulies A., Pruvost J., Rousseau B., Legrand J., Pilon L. (2016b) Simple method for measuring the spectral absorption cross-section of microalgae. Chemical Engineering Science 146, 357–368

Kerker M. (1982) Lorenz–Mie scattering by spheres: some newly recognized phenomena. Aerosol Science and Technology 1, 275–291

Kirk J.T.O., Goodchild D.J. (1972) Relationship of photosynthetic effectiveness of different kinds of light to chlorophyll content and chloroplast structure in green wheat and ivy leaves. Australian Journal of Biological Sciences 25, 215–241

Kong B., Vigil R.D. (2014) Simulation of photosynthetically active radiation distribution in algal photobioreactors using a multidimensional spectral radiation model. Bioresource Technology 158, 141–148

Krekov G.M., Krekova M.M., Lisenko A.A., Sukhanov A.Ya. (2009) Radiative characteristics of plant leaf. Atmospheric and Oceanic Optics 22, 241–256

Lichtenthaler H.K. (1987). Chlorophylls and carotenoids: pigments of photosynthetic biomembranes. Methods in Enzymology 148, 350 – 382

Lork W., Fukshansky L. (1985) The influence of chlorophyll fluorescence on the light gradients sand the phytochrome state in a green model leaf under natural conditions. Plant, Cell and Environment 8, 33–39

Ma C.Y., Zhao J.M., Liu L.H. (2018) Experimental study of the temporal scaling characteristics of growth-dependent radiative properties of *Spirulina platensis*. Journal of Quantitative Spectroscopy and Radiative Transfer 217, 453–458

Ma C.Y., Zhao J.M., Liu L.H., Zhang L. (2019) Growth-dependent radiative properties of Chlorella vulgaris and its influence on prediction of light fluence rate in photobioreactor. Journal of Applied Phycology 31, 235–247

Merzlyak M.N., Chivkunova O.B., Zhigalova T.V., Naqvi K.R. (2009) Light absorption by isolated chloroplasts and leaves: effects of scattering and 'packing'. Photosynthesis Research 102, 31–41

Nara M., Shiraiwa Y., Hirokawa T. (1989) Changes in the carbonic anhydrase activity and the rate of photosynthetic O_2 evolution during the cell cycle of *Chlorella ellipsoidea* C-27. Plant Cell Physiology 30, 267–275

Nauha E.K., Alopaeus V. (2013) Modeling method for combining fluid dynamics and algal growth in a bubble column photobioreactor. Chemical Engineering Journal 229, 559–568

Nauš J., Lazár D., Baránková B., Arnoštová A. (2018) On the source of non-linear light absorbance in photosynthetic samples. Photosynthesis Research 136, 345–355

Nedbal L., Trtílek M., Červená J., Komárek O., Pakrasi H.B. (2008) A photobioreactor system for precision cultivation of photoautotrophic microorganisms and for high-content analysis of suspension dynamics. Biotechnology and Bioengineering 100, 902–910

Otsuka H., Morimura J. (1966) Change of fatty acid composition of *Chlorella ellipsoidea* during its cell cycle. Plant and Cell Physiology *7*, 663–670

Paillotin G., Leibl W., Gapiński J., Breton J., Dobek A. (1998) Light gradients in spherical photosynthetic vesicles. Biophysical Journal 75, 124–133

Pilon L., Berberoğlu H., Kandilian R. (2011). Radiation transfer in photobiological carbon dioxide fixation and fuel production by microalgae. Journal of Quantitative Spectroscopy & Radiative Transfer, 112, 2639 – 2660

Pilon L., Kandilian, R. (2016) Interaction between light and photosynthetic microorganisms. In: Legrand J. (ed.) Advances in Chemical Engineering, Photobioreaction Engineering, 107–149

Pottier L., Pruvost J., Deremetz J., Cornet J.-F., Legrand J., Dussap C.G. (2005) A fully predictive model for one-dimensional light attenuation by *Chlamydomonas reinhardtii* in a torus photobioreactor. Biotechnology and Bioengeneering 91, 569–582

Quirantes A., Bernardt S. (2006) Light-scattering methods for modelling algal particles as a collection of coated and/or nonspherical scatterers. Journal of Quantitative Spectroscopy & Radiative Transfer 100, 315–324

Reynolds, E. (1963). The use of lead citrate at high pH as an electron-opaque stain in electron microscopy. Journal of Cell Biology 17, 208–212

Schreiber C., Behrendt D., Huber G., Pfaff C., Widzgowski J., Ackermann B., Müller A., Zachleder V., Moudříková Š., Mojzeš P., Schurr U., Grobbelaar J., Nedbal L. (2017) Growth of algal biomass in laboratory and in large-scale algal photobioreactors in the temperate climate of western Germany. Bioresource Technology 234, 140–149

Semenenko V.E., Zvereva M.G. (1972) Comparative study on the modification of photobiosynthesis direction in two *Chlorella* strains during decoupling of cellular functions by extreme temperature. Fyziologia Rastenii 19, 229–238 (in Russian)

Seyfried M., Fukshansky L. (1983) Light gradients in plant tissue. Applied Optics 22, 1402–1408

Sorokin C. (1957) Changes in photosynthetic activity in the course of cell development in Chlorella. Physiologia Plantarum 10, 659–666

Sorokin C. (1959). Tabular comparative data for the low-and high-temperature strains of *Chlorella*. Nature 184, 613–614

Sušila P., Nauš J. (2007) A Monte Carlo study of the chlorophyll fluorescence emission and its effect on the leaf spectral reflectance and transmittance under various conditions. Photochemical and Photobiological Sciences 6, 894–902

Takeda H., Hirokawa T. (1978) Studies on the cell wall of Chlorella I. Quantitative changes in cell wall polysaccharides during the cell cycle of *Chlorella ellipsoidea*. Plant and Cell Physiology 19, 591–598

Treves H., Raanan H., Finkel O.M., Berkowicz S.M., Keren N., Shotland Y., Kaplan A. (2013) A newly isolated *Chlorella* sp. from desert sand crusts exhibits a unique resistance to excess light intensity. FEMS Microbiology Ecology 86, 373–380

Treves H., Raanan H., Kedem I., Murik O., Keren N., Zer H., Berkowicz S.M., Giordano M., Norici A., Shotland Y., Ohad I., Kaplan A. (2016) The mechanisms whereby the green alga *Chlorella ohadii*, isolated from desert soil crust, exhibits unparalleled photodamage resistance. New Phytologist 210, 1229–1243

Uličný J. (1992) Lorenz-Mie light scattering in cellular biology. General Physiology and Biophysics 11**,** 133–151

Watté R., Aernouts B., Van Beers R., Herremans E., Ho Q.T., Verboven P., Nicolaï B., Saeys W. (2015) Modeling the propagation of light in realistic tissue structures with MMC-fpf: a meshed Monte Carlo method with free phase function. Optics Express 23, 17472

Westerwalbesloh C., Brehl C., Weber S., Probst C., Widzgowski J., Grünberger A., Pfaff C., Nedbal L., Kohlheyer D. (2019) A microfluidic photobioreactor for simultaneous observation and cultivation of single microalgal cells or cell aggregates. PLoS ONE 14, e0216093

Wheaton Z.C., Krishnamoorthy G. (2012) Modeling radiative transfer in photobioreactors for algal growth. Computers and Electronics in Agriculture 87, 64–73

Witkowski K., Król T., Łotocka M. (1994) The light scattering matrix of *Chlorella vulgaris* cells and its variability due to cell modification. Oceanologia 36, 19–31

Witkowski K., Król T., Zieliński A. Kuteń E. (1998) A light-scattering matrix for unicellular marine phytoplankton. Limnology and Oceanography 43, 859–869

Witkowski K., Woliński L., Turzyński Z., Gędziorowska D., Zieliński A. (1993) The investigation of kinetic growth of *Chlorella vulgaris* cells by the method of integral and dynamic light scattering. Limnology and Oceanography 38, 1365–1372

Zhao J.M., Ma C.Y., Liu L.H. (2018) Temporal scaling of the growth dependent optical properties of microalgae. Journal of Quantitative Spectroscopy and Radiative Transfer 214, 61–70